Published in Forest Ecology and Management 242 (2007) 756 – 763.

Estimation of leaf area index in eucalypt forest with vertical foliage: using cover and fullframe fisheye photography

Craig Macfarlane[1*], Andrew Grigg[2] and Crystelle Evangelista[2]

[*] Corresponding author, Phone: +61 8 6488 7924, Fax: +61 8 6488 7925, cmacfarl@cyllene.uwa.edu.au

[1] Ecosystems Research Group, School of Plant Biology (M090) and Centre for Excellence in Natural Resource Management, Faculty of Natural and Agricultural Sciences, The University of Western Australia, 35 Stirling Highway, Crawley, W.A. 6009, Australia.

[2] Alcoa World Alumina Australia, PO Box 172, Pinjarra W.A. 6208, Australia.

Keywords: hemispherical photography, light extinction coefficient, *Eucalyptus marginata*, foliage cover, stand density, leaf area index

Suggested reviewers

Cescatti A. Centro di Ecologia Alp ina, Viote del Monte Bondone, I-38040 Trento, Italy. cescatti@cealp.it

Jonckheere I. Katholieke Universiteit Leuven, Department of Land Management, Laboratory for Forest, Nature and Landscape Research, VitalDecosterstraat, 102, 3000 Leuven, Belgium. inge.jonckheere@agr.kuleuven.ac.be

Leblanc S. Natural Resources Canada/Canada Centre for Remote Sensing, 6767 Route de l'ae´roport, St-Hubert, Que., Canada J3Y 8Y9. Sylvain.Leblanc@CCRS.NRCan.gc.ca

Wagner S. Dresden University of Technology, Chair of Silviculture, Pienner Str. 8, D-01735 Tharandt, Germany. wagner@forst.tu-dresden.de

Zhang Y. University of Toronto, 100 St. George St., Room 5047 Toronto, Ont. Canada M5S 3G3. zhangy@geog.utotonto.ca

Abstract

This study compared two novel indirect methods for estimating leaf area index (*L*) in broad leaved forest, fullframe fisheye photography and cover photography, with circular fisheye photography and destructive *L* estimation. Fullframe fisheye photography differs from circular fisheye photography in that the images have reduced field of view such that the zenithal range of 0° to 90° extends to the corners of the rectangular image, roughly doubling image resolution compared to circular fisheye images. Cover images instead are obtained by pointing a 70 mm equivalent focal length lens (in 35 mm format) straight upwards. Cover and *L* were measured in twelve stands of 17 year old *Eucalyptus marginata* forest that had been planted at four initial densities: 625, 1250, 2500 and 10000 trees per hectare. *L* from destructive sampling averaged between 2 and 2.4 for stands planted at between 1250 and 10000 trees ha^{-1} but was only 1.3 for the stands planted at 625 trees ha^{-1}. Cover photography provided good indirect estimates of *L* assuming a spherical leaf distribution, except in the stands with 10000 trees ha^{-1}. These trees appeared to have a more horizontal leaf angle based on the calculated zenithal extinction coefficient for those stands (~0.7). Rapid and automated analysis of cover images using WinSCANOPY 2006 yielded similar results to manual image analysis using PhotoShop 7.0. Estimates of *L* from fullframe fisheye photography were better correlated with *L* from destructive sampling than *L* estimated from circular fisheye photography, but neither performed as well as cover photography. Photographic methods that use a single threshold to separate sky and foliage appear less sensitive to the camera's gamma function than methods that use a two-value threshold. Gamma describes the relation between actual light intensity during photography and the brightness value of the pixel. Higher resolution (>10 megapixel) cameras and better lenses, may further improve *L* estimation using fullframe fisheye photography. We recommend that cover photography be used for routine *L* estimation in eucalypt forest until it is demonstrated that fisheye methods can provide similar accuracy.

1. Introduction

Despite the well-established importance of leaf area index (*L*) for modelling plant growth and water use, indirect methods for measuring it are poorly developed. Harvesting of trees for direct measurement of leaf area is labour intensive, time-consuming, destructive, and sometimes impractical or dangerous owing to poor access and rugged terrain (Chen et al., 1997; Kucharik et al., 1999; Macfarlane et al., 2000; Bréda, 2003; Macfarlane et al., 2006). With the release of affordable digital cameras, fisheye photography (Anderson, 1964) has

become a rapid and cheap method for estimating *L*. However, fisheye photography is sensitive to photographic exposure, the gamma function of the film or camera, method of pixel classification and image resolution (Chen et al., 1991; Blennow, 1995; Macfarlane et al., 2000; Wagner, 2001; Jonckheere et al., 2005; Cescatti, 2006; Macfarlane et al., 2006; Wagner and Hagemeier, 2006).

The importance of exposure control is well documented (Chen et al., 1991; Macfarlane et al., 2000; Zhang et al., 2005) and the two-value threshold method has been proposed as a means of reducing the effects of exposure on L_t derived from fisheye photographs (Wagner, 2001). Macfarlane et al. (2006) showed that large errors can result from analysing fisheye images using a two-value threshold if the images are not corrected for the gamma function of the camera; Wagner (1998) illustrated the importance of correcting images for the gamma function of chemical films when using the two-value threshold method. The gamma function of a digital camera describes the relation between the actual light intensity during photography and the resulting brightness value of the pixel (Wagner, 1998; Cescatti, 2006) ; an image that accurately reproduces actual light intensities would have a gamma value of 1.0. Digital cameras typically have gamma values between 2 and 2.5 (Cescatti, 2006) ; Leblanc (2006) found that the most popular camera used for digital fisheye photography, the Nikon Coolpix 4500, has a gamma function of 2.2, and Macfarlane et al. (2006) obtained good results using this gamma value. The importance of variations in the gamma function have not been investigated for single threshold pixel classification methods.

In theory, by measuring the gap fraction at multiple zenith angles it is theoretically possible to simultaneously determine both *L* and the foliage angle distribution, and this should be the biggest advantage of fisheye methods. However, similarly to previous studies (Chen and Black, 1991), Macfarlane et al. (2006) found that the foliage angle distribution calculated from fisheye photography was as much affected by canopy structure as by the actual foliage angle distribution, despite corrections for foliage clumping. It is possible that this is the result of the lower resolution of fisheye images and resulting poorer estimates of crown porosity obtained from fisheye images; Blennow (1995) observed that higher resolution images have fewer “mixed pixels”, which could obscure small gaps within canopies resulting in underestimation of canopy porosity and calculation of an inaccurate gap size distribution. The resolution of fisheye images can be easily improved by using fullframe fisheye images instead of circular images. Unlike circular images, in which the entire canopy hemisphere (zenithal range of 0 to 90°) is contained in a circle that occupies about half the pixels inside a

rectangular image, fullframe fisheye images have a reduced field of view such that the zenithal range of 0° to 90° extends to the corners of the rectangular image, roughly doubling image resolution. The ability to apply the same gap fraction inversion methods applied to circular fisheye images to fullframe images has only recently been implemented in WinSCANOPY 2006. Potentially, this greatly increases the range of cameras and lenses that can be used for fisheye photography. Previously, digital hemispherical photography was largely limited to the Nikon Coolpix range of cameras and their fisheye converters, or a very few expensive digital SLR cameras with 35 mm CMOS or CCD, and the few 8 mm fisheye lenses that were available.

As another alternative to circular fisheye photography, Macfarlane et al. (2006) tested digital photographic images of the canopy obtained by pointing a 70 mm equivalent focal length lens (in 35 mm format) upwards to estimate crown cover (% ground covered by the vertical projection of solid crowns) and foliage cover (% ground covered by the vertical projection of foliage and branches). After correcting for foliage clumping they estimated *L* from the Beer-Lambert law. The method outperformed fisheye photography in that study (Macfarlane et al., 2006) and had many advantages over fisheye photography; it could be applied during daylight hours, cover images were much higher resolution than fisheye images and, thus, less sensitive to photographic exposure; sky luminance was more even, and the narrow viewing angle and rectangular shape of the cover images was better suited to small rectangular experimental plots. The disadvantages of the method were that the image analysis was not automated, although it was simple and rapid, and the method required an assumed zenithal light extinction coefficient (*k*). An automated method of analysing cover images has recently been incorporated in WinSCANOPY 2006 (Regent Instruments, Ste-Foy, Quebec). Unlike the colour-based pixel classification used by Macfarlane et al. (2006), WinSCANOPY uses a single threshold to separate sky from foliage and then analyses the resulting black and white image. The effect of the gamma function on *L* estimates from cover photography has not been investigated.

The main objectives of this study were to compare fullframe fisheye photography with circular fisheye photography, cover photography and destructive *L* estimation, and to quantify the effect that variations in the gamma function have on *L* estimated from single threshold photographic methods. Unlike the study of Macfarlane et al. (2006) in which three different *L*s were obtained by thinning a single stand, in this study we compared *L* estimates from

twelve independent stands that varied in stand density and *L*. We expected that cover photography and fullframe fisheye photography would provide better estimates of *L* than circular fisheye photography owing to their superior image resolution, and that fullframe fisheye photography would provide better estimates of the leaf angle distribution and clumping index than circular fisheye photography. We also expected that converting the gamma of images from the Nikon Coolpix 4500 back to 1.0 from 2.2 would decrease the calculated gap fraction and provide more accurate estimates of *L*.

Other objectives of this study were:

1) to compare the manual, colour-based analysis of cover images with PhotoShop used by Macfarlane et al. (2006) with the automated, single threshold analysis implemented in WinSCANOPY 2006.

2) to compare leaf area of individual trees from destructive sampling against estimates using the equations developed by Whitford (1991). The empirically derived equations, developed in mature jarrah forest rather than young regrowth, use measurements of tree diameter and crown attributes, and provide a tool to estimate *L* that is intermediate in effort between full destructive harvesting and indirect photographic methods.

2. Materials and Methods

2.1. Study sites

The present work was conducted in a subset of experimental plots established in 1988 to investigate the growth patterns of jarrah (*Eucalyptus marginata*) in rehabilitated bauxite mine pits (Ward and Koch, 1995; Koch and Ward, 2005). In each of three pits at Scribbly Road (ScR), Karri Road (KR) and Scarp North (SN), 100 jarrah seedlings had been planted at four spacings: 1×1, 2×2, 2×4 and 4×4 m, giving initial stand densities of 10000, 2500, 1250 and 625 stems/ha. Plot size varied according to spacing, with dimensions of 10×10, 20×20, 40×20 and 40×40 m. Each plot had been seeded with understorey species containing no large *Acacias* and Superphosphate No. 1 fertiliser was applied at 500 kg ha^{-1}. Plots se 1 lected for this study were also treated with a 200g tablet of diammonium phosphate per tree.

2.2. Crown assessment and tree harvesting for allometric L estimation

The diameter at breast height (1.3 m) over bark (*D*) of all trees in the innermost eight rows of the twelve plots was measured in December 2005. In January-February 2006, four or five trees, which represented the range of tree diameters in the plot, were felled in each of eight

8 plots (two plots from each density treatment) over a period of several weeks. At Scarp North,
9 a further two trees were felled from the 2×4 treatment but none from the 4×4 m treatment
10 because these stands were destroyed by wildfire in February 2006, before destructive
11 sampling was completed. No trees were harvested from the 1×1 and 2×2 m treatments at
12 Karri Rd because of poor site access. Prior to felling, *D* of each tree was remeasured, and
13 bark depth, crown dimensions (tree height, crown depth and crown width) and subjective
14 crown assessments (objective density, Grimes density, Grimes crown size and fruiting status)
15 were made as described by Whitford (1991). Crown area (CA) was calculated from crown
16 width (CW) and crown depth (CD) as CA = CW×CD, and crown volume (CV) was calculated
17 assuming that the crown was shaped like an ellipsoid, $CV = \pi/12 \times CW_2 \times CD$.
18
19 After each tree was felled, its total height and the height to the base of the live crown were
20 remeasured, and the tree's branches were removed. Individual stems of trees that forked
21 below 1.3 m height were treated as separate trees. Any branches with a diameter larger than
22 15 mm were stripped of smaller branches so that all branches had a diameter less than 15 mm.
23 On the basis of a visual assessment of their diameter, the branches were separated into three
24 groups (large, medium and small) and weighed. A subsample of branches from each group
25 (more than 30 % of the total mass) were immediately reweighed and stripped of leaves. The
26 area of leaves from each subsample was measured with a calibrated leaf area meter. The ratio
8of leaf area to fresh branch mass of the sample branches was used to calculate 1 the leaf area of
2 all the branches in that size class. These were summed for each sample tree to estimate its
3 total leaf area. The ratio method of estimating individual tree leaf areas has the advantage that
4 the estimate of tree leaf area is constrained by the known total canopy mass (Snowden, 1986),
5 and the error in the estimation of the ratio of leaf area to total branch mass is small if at least
6 30 % of branches are sampled (Snowden, 1986).
7
8 Plots of tree leaf area *versus D* were noticeably curvilinear and heteroscedascic. We tested
9 both square root and logarithmic transformations of the data. For logarithmic regressions
10 both the dependent and independent variable were natural log transformed, but only the
11 dependent variable leaf area was square root transformed because this was adequate to
12 achieve linear, homoscedascic relationships of leaf area to *D* in this case. The smallest tree
13 was removed from statistical analyses of the natural log transformed data because of the large
14 influence that it had on these regressions. This tree had *D* less than 7 cm, a leaf area of 0.2 m_2
15 and was less than 3.5 m tall. Analysis of covariance was used to test whether the slope and
16 intercept of regressions differed between different treatments (tree spacings), and was

17 calculated using the ordinary least squares method.
18
19 It has been suggested that standardized or reduced major axis regression (RMA) is preferable
20 to ordinary least squares regression for calculating regressions between different components
21 of biomass because of the structural nature of the relationships. However, we judged that
22 ordinary least squares regression was more appropriate because 1) the X-axis variable, *D*, is
23 generally measured much more accurately than leaf area; McArdle (1988) suggested that
24 ordinary least squares regression was preferred unless the error in the independent variable
25 was more than one-third of that of the dependent variable; and 2) the purpose was to derive an
26 equation to predict leaf area from measurements of tree diameter that contain measurement
9 error (Warton et al., 2006). All regressions of leaf area *versus D* were corrected 1 for bias using
2 Snowden's (1991) bias correction factor, which was then applied to all trees in each stand and
3 their leaf areas summed to obtain *L* of each stand.
4
5 *2.3. Photographic methods and image analysis*
6 All digital photographs were collected as FINE JPEG images with maximum resolution
7 (3,871,488 pixels total) using a Nikon Coolpix 4500 camera. Cover images (Macfarlane et
8 al., 2006) were collected during the afternoon on a grid in each plot. Nine images were
9 collected from the 1×1 and 2×2 m plots, twelve images from the 2×4 m plots and 16 from the
10 4×4 m plots. The camera, without fisheye converter, was set to F2 lens, automatic exposure,
11 Aperture-Priority mode and minimum aperture (*f*/9.6). The lens was pointed directly upwards
12 and the camera lens was levelled using a bubble level fixed to an aluminium plate fitted
13 between the camera tripod mount and tripod.
14
15 Cover images were analysed using Adobe PhotoShop 7.0 as described by Macfarlane et al.
16 (2006) and also using WinSCANOPY Pro 2006a (Regent Instruments, Ste-Foy, Quebec).
17 Images from the Nikon Coolpix 4500 have an approximate gamma function of 2.2 applied to
18 them by the camera's inbuilt software (Leblanc, 2006). For analysis by WinSCANOPY Pro
19 2006a we also generated a set of images that were back-corrected to a gamma function of 1.0
20 using IrfanView 3.95 (©1996-2004 by Irfan Skiljan); the original images were batch
21 converted with the gamma correction set to 0.45 (1/2.2).
22
23 In PhotoShop images were analysed in colour; large, between-canopy gaps were visually
24 selected by the operator using the "Wand" tool and the number of pixels recorded from the
25 Histogram. All sky pixels (those with similar colour and luminance characteristics to the

26 large gaps) were selected using the Select Similar command and the total sky pixels recorded.
10
In WinSCANOPY the blue channel of the sharpened (medium) RGB 1 images was analysed.
2 Sky pixels were separated from canopy pixels using a threshold brightness value that was
3 automatically determined by algorithms within the software. WinSCANOPY separated large
4 gaps from small gaps based on their area; gaps larger than 50,000 pixels (1.3 % of the total
5 image area) were arbitrarily classified as large gaps. This threshold gap size was selected
6 based on experience from image analyses using the PhotoShop method. Both the PhotoShop
7 and WinSCANOPY derived data were used to calculate foliage cover (f_f), crown cover (f_c),
8 crown porosity (Φ, eq. 1), plant area index (L_t, eq. 2) and zenithal clumping index ($\Omega(0)$, eq.
9 3) after Macfarlane et al. (2006). No corrections were made for woody area for any of the
10 photographic methods. Hence, indirect estimates of L are referred to as plant area index (L_t).
11 In WinSCANOPY all calculations were performed automatically, while for data derived from
12 PhotoShop calculations were performed using Microsoft Excel.
13
14 $\Phi = 1 - f_f/f_c$ (1)
15 $L_t = -f_c \ln(\Phi) / k$ (2)
16 $\Omega(0) = (1-\Phi) \ln(1- f_f) / \ln(\Phi) / f_f$ (3)
17
18 For calculation of L from cover images we assumed a light extinction coefficient (k) at the
19 zenith of 0.5. For comparison we also calculated k using equation 4, from crown cover (f_c), Φ
20 and L estimated from destructive sampling.
21
22 $k = -f_c \ln\Phi / L$ (4)
23
24 Four circular fisheye images and four fullframe fisheye images were collected at sunset near
25 the centre of each plot using the Coolpix 4500 with FC-E8 fisheye conversion lens. The lens
26 was set to F1 for circular images and F2 for full-frame images. The camera was pointed
directly upwards and levelled as for cover photography. Aperture 1 was set to its minimum
2 (f/5.3 for circular images and f/9.6 for full-frame images) to minimise lens vignetting and,
3 with the camera set to Manual mode, shutter speed was set to over-expose each image by one4
stop, as metered beneath the canopy. This exposure setting provided good contrast between
5 canopy and sky based on an examination of the greyscale histogram.
6
7 Fisheye images were analysed using DHP 4.2.2 and TRACWin 3.7.3 (Leblanc, 2006), and

8 using WinSCANOPY Pro 2006a (Regent Instruments, Ste-Foy, Quebec). DHP uses a two9 value, regional threshold method to classify images; the threshold is selected interactively by 10 the software and user. Images were analysed by DHP-TRACWin as described by Macfarlane 11 et al. (2006) with a gamma setting of 2.2 to account for the camera's gamma function. 12 WinSCANOPY uses a single global threshold that is automatically determined by the 13 software's own algorithms. As for cover image analysis, we also generated a set of images 14 that were back-corrected to a gamma function of 1.0 using IrfanView 3.95. Both the original 15 and corrected images were analysed using WinSCANOPY to test the effect of gamma 16 correction on estimates of *L* using the single threshold method.

17

18 The blue channel of all RGB images was sharpened (medium) and analysed using 19 WinSCANOPY with a sky grid comprising of seven zenithal rings from 0 to 70° and eight 20 azimuthal regions. WinSCANOPY calculated L_t from both "linearly-averaged" and "log21 averaged" (Lang and Xiang, 1986) gap fractions within each zenith and azimuth region, using 22 both the generalised Licor LAI-2000 method (Welles and Norman, 1991), and the ellipsoidal 23 method (Campbell, 1986); the ellipsoidal method was also used to calculate the mean leaf 24 angle from log-averaged gap fractions. L_t from the Licor and ellipsoidal methods were 25 averaged. A mean clumping index was calculated as the ratio of L_t from the linear- to the log averaging method. The gap fraction distribution was also corrected for foliage clumping using the gap size distribution method (Chen and Cihlar, 1 1995; Leblanc, 2002). We have 2 abbreviated the Lang and Xiang (1986) method as LX, the Chen and Cihlar method (1995) as 3 CC and the combined method as CLX following the convention introduced by Leblanc et al. 4 (2005). Where no correction has been applied for clumping we have used the abbreviation 5 NC.

6

7 Both uncorrected (gamma = 2.2) and corrected (gamma = 1.0) images were also analysed 8 using Hemiview 2.1 (Delta-T Devices, Cambridge, UK). Hemiview analyses grey-scale 9 images across a zenith range from 0 to 90°, applies no clumping correction and requires a 10 single binary threshold be selected by the user.

11

12 *2.4. Statistical Analyses*

13 Estimates of *L* from destructive sampling were initially compared with L_t from photography 14 based on the root mean-squared error (RMSE). Methods with a small RMSE were then 15 compared using RMA regression because we judged that the measurement errors were similar 16 in both approaches (McArdle, 1988) and the purpose was to test whether the true slope of the

relation was equal to one, rather than to predict Y from X (Warton et al., 2006). RMA regression was also used to compare other methods where it was judged appropriate. RMA regressions were calculated using PAST 1.40 (Hammer et al., 2001). PAST 1.40 was also used to calculate OLS regressions where it was desirable to test whether the slope of the regression differed from one. All other statistical analyses were performed using Minitab release 13.1 (Minitab Inc. State College, PA, USA). Forwards and backwards stepwise regression was used to identify crown variables that were good predictors of tree leaf area; the alpha value to enter and remove was set to 0.05. Tukey's pairwise comparison test with a family error rate of 0.05 was used to compare the four tree spacing treatments, if one-way

ANOVA indicated that a significant difference existed between them 1 in the variable of interest.

3. Results

3.1. L from tree harvesting and regression

Correlation coefficients (R^2) of tree leaf area (A_L, m^2) versus diameter at breast height over bark (D, cm) for individual treatments ranged from as little as 0.33 for the logarithmic regression for the widest spaced trees to 0.77 for some regressions of the 2×4 and 2×2 m spaced trees; R^2 of the regressions for data pooled from all treatments were 0.62 for square root transformed data and 0.70 for the logarithm transformed data. Bias correction factors (BCF) were smaller for square root regressions than for logarithmic regressions, but, otherwise, there were no clear advantages of one data transformation over the other. Analysis of covariance indicated that the slopes and intercepts of the regressions did not differ between pits or tree spacings, despite an apparent trend of decreasing slope and increasing intercept in the logarithmic regressions as tree spacing increased. No such trend was evident in the square root regressions. We used the logarithmic regression of pooled data (Equation 5) to calculate tree leaf areas and stand L.

$$\ln A_L = 2.32 \ln D - 4.22 \quad (n = 49, R^2 = 0.70, P < 0.001, BCF = 1.10) \quad (5)$$

L ranged from 0.85 to 2.83 and basal area ranged from 17 to 67 $m^2\ ha^{-1}$ (Table 1). Tree height ranged from 9 to 14 m in the 2×2, 2×4 and 4×4 spaced stands, but was only 3 to 10 m in the 1×1 m stands. One-way ANOVA and Tukey's test indicated that the stands with the widest spaced trees had a smaller L than the other three treatments ($P < 0.05$), which did not differ. L did not differ statistically between pits (one-way ANOVA).

Many of the crown dimensions and crown assessments were also well correlated with tree leaf area but, based on stepwise regression, crown area (CA) and Grimes density (GD) were the best combined estimators of leaf area, while crown width (CW), crown depth (CD) and Grimes density were the best combined estimators of the square root of leaf area. Objective density was highly correlated with Grimes density but Grimes density was always a better predictor of leaf area. Whitford (1991) also found that crown width, crown depth and Grimes density were good predictors of jarrah tree leaf area. We tested equations (ii), (iii), (iv), (vii), (viii) and (ix) from Whitford (1991) against our dataset of tree leaf area (Table 2). Plots of all data were noticeably heteroscedascic. Equation (ii), which contained only diameter under bark at 1.3 m height, performed the best based on its small intercept, slope of nearly one, good correlation coefficient and small root mean-squared error (RMSE). Including crown dimensions or crown assessments in the regressions actually appeared to make the estimates of tree leaf area worse (Table 2). Of the regressions that did not include DUB, leaf area from equation (vii) provided the best estimates of actual tree leaf area. Leaf area estimated from equation (viii) was most highly correlated with actual tree leaf area, but this equation significantly overestimated leaf area.

3.2. L and canopy characteristics from photography

Based on an initial assessment of the RMSE, the best estimates of *L* obtained from each type of image were:

1) cover photography (θ = 0-15°) using the manual PhotoShop method with gamma = 2.2 and the CC clumping correction (RMSE = 0.44, Table 3).

2) fullframe fisheye photography (θ = 0-70°) using the automated WinSCANOPY method with gamma = 2.2 and the LX clumping correction (RMSE = 0.43, Table 3).

3) circular fisheye photography (θ = 0-70°) using the automated WinSCANOPY method with gamma = 2.2 and the LX clumping correction (RMSE = 0.46, Table 3).

Generally, similar RMSE were obtained from fisheye images using WinSCANOPY regardless of whether the images were gamma corrected or not, whether they were circular or fullframe, and regardless of which clumping correction (if any) was used; with the exception that the CLX clumping correction produced noticeably worse results (Table 3). In contrast, a small RMSE was only obtained from DHP-TRACWin with the CLX clumping correction (Table 3) and was largely unaffected by the zenith angle range used. Using WinSCANOPY,

8 images with gamma = 2.2 appeared less sensitive to the choice of clumping correction than
9 images with gamma = 1.0, and fullframe fisheye images appeared less sensitive to the CC and
10 CLX clumping methods than circular images (Table 3). Poor results were obtained from
11 Hemiview.
12
13 Analytical methods with RMSE less than or equal to 0.50 were examined in more detail using
14 RMA regression (Table 4) and data from three of the regressions are presented in Figure 1 for
15 inspection. From the regressions it was clear that the cover method outperformed the fisheye
16 methods, based on its strong correlation with *L* from allometry, slopes that did not differ from
17 one and intercepts that did not differ from zero. The manual PhotoShop method performed
18 marginally better than the automated WinSCANOPY method. The fullframe fisheye method
19 generally outperformed the circular fisheye method based on its good correlation with *L* from
20 allometry, and its slopes closer to one and intercepts closer to zero than the circular fisheye
21 methods. The best results were obtained from WinSCANOPY using the LX clumping
22 correction followed by no clumping correction at all. L_t from the DHP-TRACWin method
23 with CLX clumping correction proved not to be very well correlated with *L* from allometry in
24 this study. The relative merits of correcting or not correcting the gamma of the images prior
25 to analysis by WinSCANOPY depended on the type of image and clumping correction used:
26 if no clumping correction was applied then the corrected image (gamma = 1.0) gave good
results for fullframe fisheye images, but if the LX clumping correction 1 was used then the
2 original image (gamma = 2.2) gave the best results.
3
4 All photographic methods generally yielded good estimates of *L* for the 4×4 m spaced trees
5 but overestimated *L* of the 1×1 m spaced trees (Table 5). The fisheye methods also
6 underestimated *L* of the 2×2 m and 2×4 m spaced trees (Table 5). *L* of two sites (KR 1×1 and
7 ScR 1×1) was consistently overestimated by all photographic methods and *L* of another two
8 sites (ScR 2×2 and ScR 2×4) was consistently underestimated by all photographic methods.
9
10 Foliage cover f_f, crown cover f_c and the zenithal clumping index $\Omega(0)$ all increased with
11 decreasing tree spacing (Table 5). $\Omega(0)$ was strongly positively correlated with foliage cover
12 ($\Omega(0) = 0.58\, f_f + 0.33$, $R^2 = 0.86$, n = 12, $P<0.001$). Crown porosity was not correlated with
13 foliage cover, but did differ significantly between treatments; more closely spaced trees
14 appeared to have more porous crowns (Table 5, Tukey's test, $P<0.05$). The zenithal
15 extinction coefficient (*k*) calculated from cover, porosity and destructive *L* was slightly less
16 than 0.5 for the 2×2, 2×4 and 4×4 m spaced trees, but nearly 0.7 for the 1×1 m spaced trees

(Table 5). Foliage cover was well correlated with L ($R^2 = 0.64$, $P = 0.002$). The correlation was greatly improved ($R^2 = 0.91$, $P < 0.001$) if the data for the 1×1 m spaced trees were removed and the data from Macfarlane et al. (2006) were included (Figure 2).

f_c of individual images ranged up to 0.84 and L_t ranged up to 5. Φ ranged from 4 % to nearly 30 %. The automated WinSCANOPY analysis of cover images performed nearly as well as the manual PhotoShop method, provided that the image's gamma was not corrected (i.e. gamma = 2.2, Tables 3 and 4). Correcting the gamma to 1.0 resulted in noticeably worse estimates of L (RMSE = 0.58, Table 3) and generally increased calculated L_t, f_f, f_c and $\Omega(0)$ but had little effect on Φ (data not presented). f_c, f_f, $\Omega(0)$ and L_t from PhotoShop and WinSCANOPY were highly correlated (Table 6). PhotoShop yielded slightly larger estimates of cover and the $\Omega(0)$ than WinSCANOPY; Φ from the two methods were not well correlated and did not differ significantly (Table 6).

To compare clumping indices and mean leaf angles of fullframe and circular fisheye images we selected the gamma = 2.2 images and the LX clumping correction, because both of these had the same gamma, small RMSE (Table 3) and good correlations with L from allometry. The fullframe and circular images gave quite different estimates of the mean clumping index across the zenith angle range 0-70° (Figure 3). Ω from the circular images was between 0.85 and 0.95 for all plots whereas Ω from fullframe images ranged from as little as 0.7 to more than one. Ω from fullframe images appeared to increase as L increased (Figure 3), as did $\Omega(0)$ from cover images ($R^2 = 0.40$, $P = 0.03$ for $\Omega(0)$ *versus* L). Although both were weakly positively correlated with L there was no correlation between Ω from fullframe fisheye images and $\Omega(0)$. The mean leaf angle estimated from circular images was about 4° larger than mean leaf angle from the full-frame images on average ($P = 0.007$, two-way ANOVA with image type and tree spacing as factors, n = 96). Mean leaf angle increased with increased tree spacing for both circular and fullframe images; the mean leaf angle from fullframe images increased from 62.8° (sem = 0.83) for the 1×1 m spaced plots to 70.1° (sem = 2.20) for 4×4 m spaced trees (two-way ANOVA). Mean leaf angles of the two intermediate tree spacings were similar (67.4° ± 1.30 for 2×2 spacing and 67.2° ± 1.67 for 2×4 m spacing).

4. Discussion

This is the first published study to evaluate fullframe fisheye photography for estimating L. We compared it to circular fisheye photography, cover photography and allometric estimates

of *L*, as well as testing Whitford's (1991) equations for predicting leaf area of jarrah trees. The cover method performed better than fisheye photography, and fullframe fisheye photography performed better than circular fisheye photography. We attribute this result to the greater image resolution of cover and fullframe fisheye images compared to circular fisheye images. The benefits of higher image resolution have been previously noted (Blennow, 1995). Using the Nikon Coolpix 4500, the fullframe fisheye images capture about two-thirds of the canopy hemisphere in 3.87 megapixels compared with circular images that capture the entire hemisphere in only about 2 megapixels. Our results could also reflect the wider footprint of fisheye images and the small size of some plots (as small as 10 × 10 m), but there was no evidence that analysing gap fractions from smaller zenith angles (16-45° using DHP-TRACWin) performed better than analysing larger zenith angles (57° using DHP10 TRACWin or 0-70° using WinSCANOPY).

We also found that variations in the gamma function had little effect on the results of photographic methods that use a single global threshold, whether fisheye or cover images. Increasing the gamma (as performed by the camera's internal software) did appear to increase the gap fraction based on the greater need for clumping corrections to estimate *L* accurately from fisheye images with gamma = 2.2. However, the effect was small compared to DHP-TRACWin, which uses a two-value, regional threshold, and which required that images be corrected for the camera's gamma function to obtain good results (Macfarlane et al. 2006); in that study correcting the gamma function increased estimates of *L* by up to 80 %. Single threshold methods may be less sensitive to the camera's gamma because the grey-levels of the pixels are not used to calculate gap fractions. Changing the gamma primarily alters the grey-levels of the pixels with intermediate brightness (Cescatti, 2006), many of which may lie between the two thresholds used by the two-value threshold method. Instead, the single threshold method converts all pixels to either black or white and appears less sensitive to modification of the grey-levels of intermediate pixels. Although the single threshold methods tested appeared insensitive to the gamma function, it would still be prudent, in the future, to

use cameras that can save files in RAW format, and not have their gamma modified. The results from this study might have been affected by the images having their gamma changed by the camera's software and then converted back using IrfanView. A better test of the effects of gamma variations would be to compare unmodified RAW format images to JPG or TIFF format images.

The findings of this study are very significant because fullframe fisheye photography allows a wider range of digital cameras and lenses to be used than those currently used. This includes cameras that can save files in RAW format unlike the Coolpix 4500, which requires complex methods to obtain RAW images (Cescatti, 2006), and permits the use of cameras that have better resolution than the Coolpix 4500 e.g. 8 - 12 megapixels digital SLR cameras; these cameras can also be used with better quality fisheye lenses. It is possible that further increases in image resolution will further improve estimates of *L*, mean leaf angles and clumping indices from fisheye photography.

L estimation from cover photography can be streamlined by using the batch analysis capability of WinSCANOPY and treating all gaps larger than 50,000 pixels (for the Nikon Coolpix 4500) as non-random, between crown gaps. WinSCANOPY also has the capacity to separate non-random gaps by applying the CC method to cover images, but this was not tested. Although results between WinSCANOPY and PhotoShop varied for individual images, as evidenced by the small correlation coefficients between the two methods for crown porosity and $\Omega(0)$, there was little difference in estimation of cover or *L* between the two methods.

Crown porosity obtained from this study (0.11-0.16) was similar to the range 0.13-0.17 obtained for 12 year old jarrah by Macfarlane et al. (2006) suggesting that crown porosity is consistent in jarrah of this age grown on revegetated mine sites. There 1 was evidence that the zenithal extinction coefficient (*k*) of jarrah crowns can be affected by tree spacing. Bolstad and Gower (1990) concluded that errors of *L* estimation were three times greater if *k* was assumed rather than measured locally, but this study has confirmed the earlier study of Macfarlane et al. (2006) that good estimates of *L* can be obtained from cover photography in jarrah forest using *k* between 0.45-0.50, except in very dense, short stands. Based on *k* at the zenith calculated from cover and *L* from allometry, it appeared that the shorter, closely spaced trees had a more horizontal leaf angle distribution ($k \sim 0.7$) than trees in the other three spacing treatments ($k \sim 0.47$). This conclusion was also supported by the smaller mean leaf angle calculated from fisheye photography for the 1×1 m spaced trees compared with the other treatments, although mean leaf angles estimated from fisheye photography need to be treated with caution (Chen and Black, 1991), even when they are corrected for the effects of foliage clumping (Macfarlane et al., 2006). The larger extinction coefficient may have resulted from shading although we can not confirm this; the closest spaced trees in the small 10×10 m plots were also the shortest trees and, as a result, at the time of sampling they were

surrounded by taller trees that had been established in wider spaced plots where there was presumably less competition for light, water and nutrients between trees during the earlier stages of growth. Other studies have reported more horizontal leaf angles in shaded plants of the same species (for example, Balaguer et al., 2001; Farque et al., 2001). We conclude that *L* of jarrah grown on rehabilitated mine sites, with the exception of very dense, short stands, can be estimated with good accuracy from foliage cover alone, either by assuming a crown porosity of ~0.14 and *k* ~0.47 or by using the regression of L_t *versus* f_f shown in Figure 2. The contribution of wood to total plant area has been ignored in this analysis, which would result in *k* at the zenith being over-estimated, but the error resulting from wood is likely to be smaller for cover images than for hemispherical-sensor based methods because stems contribute little to the cover 'seen' by an upward looking, narrow angle 1 lens (Kucharik et al., 1998).

This study confirmed that the CLX clumping correction is needed to obtain the best results from DHP-TRACWin, as found by Macfarlane et al. (2006) and Leblanc et al. (2005). In contrast, the LX method should be preferred if using WinSCANOPY, although this may depend on the gamma of the images being analysed. Previous studies (e.g. van Gardingen et al., 1999) also found that LX method improves estimates of *L* in clumped canopies. The LX method is only sensitive to the overall gap fraction, not to the gap size distribution, and may provide more robust estimates of Ω in situations where the gap size distribution is inaccurate owing to the effects of photographic exposure, camera gamma function and image resolution. The good performance of the LX method (which generally gives comparable results to the CC method) from fisheye photography using WinSCANOPY, and the good results obtained from the CC method from cover photography, together suggest that the amount of correction for foliage clumping from these two methods is about right. Macfarlane et al. (2006) questioned whether the clumping indices given by the CLX method were realistic, especially when calculated Ω was still quite small at zenith angles such as 57°. We suggest that the good results obtained from DHP-TRACWin using the CLX method may indicate compensating errors within that approach that relate to either the calculated gap fraction or foliage angle distribution.

Canopy dimensions such as crown width and depth, and subjective crown assessments such as Grimes density, were well correlated with the leaf area of individual jarrah trees, but Whitford's (1991) equations that contained these variables did not predict tree leaf area as well as tree diameter. Whitford's (1991) equation (ii) yielded estimates of tree leaf area from

diameter under bark that were unexpectedly accurate given that the trees sampled by Whitford (1991) were taken from natural forest and were up to three times taller than the trees sampled in this study. This study appears to support the use of equation (ii) to indirectly estimate leaf area of jarrah trees regardless of the age, size or growth rate of the trees, which is surprising given that allometric equations are expected to be climate, age and stand density specific (Menucuccini and Grace, 1995; Le Dantec et al., 2000). Estimates of leaf area based on crown dimensions could also be expected to be site or age independent, but did not perform well in this study. This may indicate that the crowns of jarrah trees from natural forest and revegetated mine sites are quite different, at least in 17 year old stands. We have measured Φ of 0.25-0.30 in 25 m tall natural jarrah forest (Macfarlane et al. unpublished data); about double the Φ found in this study, which supports this conclusion. Even so, there is no clear evidence from the regressions in Table 2 that the less porous crowns of jarrah trees in this study resulted in consistent underestimation of leaf area from Whitford's (1991) equations as might have been expected, although several regressions did have slopes less than one. Overall, we must disagree with Whitford's (1991) conclusion that crown assessments improve regression estimates of leaf area in jarrah trees, at least on revegetated mine sites.

5. Conclusions

We conclude that, while fullframe fisheye photography holds the greatest promise for achieving the "Holy Grail" of accurate and simultaneous estimation of L, foliage angle distribution and foliage clumping, cover photography is currently the best option for routine, indirect measurement of L in broadleaf forests. The most disturbing aspect of fisheye photography is the bewildering array of leaf area estimates and Ω estimates that can be produced by different software packages, and within the same software package, using different thresholding methods and different methods of correcting for foliage clumping. Wagner and Hagemeier (2006) also reported that the method of pixel segmentation caused variations in the calculated leaf angle distribution. The somewhat unpredictable sensitivity of fisheye photography to other factors such as the camera's gamma function and photographic exposure adds further uncertainty to the methods. This study has identified methods within two software packages that appear to give reasonable results. However, there is no obvious *a priori* reason for choosing these methods ahead of several others that performed more poorly. We conclude that the apparent advantage of fisheye photography, that L and k are simultaneously estimated, is largely unrealised in practice. Furthermore, fisheye photography

can only be applied in certain sky conditions, usually near sunrise or sunset when the sky brightness is uniform, which is a significant occupational health and safety risk for employees who must work during non-daylight hours in remote locations, sometimes in rough terrain. As a consequence, it is the authors' experience that the methods are frequently applied in inappropriate sky conditions and measurements may be of poor quality. In contrast, cover photography is relatively insensitive to photographic exposure and the camera's gamma function, is easily automated, and yields unequivocal, testable results. *k* at the zenith can be measured when the opportunity arises. Of course, further testing of cover photography is necessary in other broadleaved forests, especially those that do not have a nearly spherical leaf distribution.

Acknowledgements

We thank the many leaf pluckers for their efforts, with special thanks to Naomi Kerp for assistance with field measurements. We thank Alcoa World Alumina Australia for access to the experimental site and tree felling services. The financial support of the Australian Research Council (Discovery grant DP0344927) to the senior author is acknowledged. We thank Regie and Regent Instruments for the speed and enthusiasm with which they incorporated analysis of cover images and fullframe fisheye images into WinSCANOPY 2006 at our request.

References

Anderson, M.C., 1964. Studies of the woodland light climate I. The photographic computation of light conditions. J. Ecol., 52, 27-42.

Balaguer, L., Martínez-Ferri, E., Valladares, F., Pérezcorona, M.E., Baquedano, F.J., Castillo, F.J. et al., 2001. Population divergence in the plasticity of the response of *Quercus coccifera* to the light environment. Funct. Ecol., 15, 124-135.

Blennow, K., 1995. Sky view factors from high-resolution scanned fish-eye lens photographic negatives. J. Atmos. Ocean Tech., 12, 1357-1362.

Bolstad, P.V. and Gower, S.T., 1990. Estimation of leaf area index in fourteen southern Wisconsin forest stands using a portable radiometer. Tree Physiol., 7, 115-124.

Bréda, N.J.J., 2003. Ground-based measurements of leaf area index: a review of methods, instruments and current controversies. J. Exp. Bot., 54, 2403-2417.

Campbell, G.S., 1986. Extinction coefficients for radiation in plant canopies calculated using an ellipsoidal inclination angle distribution. Agric. Forest Meteorol., 36, 317-321.

15 Cescatti, A., 2006. Indirect estimates of the canopy gap fraction based on the linear
16 conversion of hemispherical photographs. Methodology and comparsion with standard
17 thresholding techniques. Agric. Forest Meteorol., in press.
18 Chen, J.M. and Black, T.A., 1991. Measuring leaf area index of plant canopies with branch
19 architecture. Agric. Forest Meteorol., 57, 1-12.
20 Chen, J.M., Black, T.A. and Adams, R.S., 1991. Evaluation of hemispherical photography for
21 determining plant area index and geometry of a forest stand. Agric. Forest Meteorol.,
22 56, 129-143.
23 Chen, J.M. and Cihlar, J., 1995. Plant canopy gap-size analysis theory for improving optical
24 measurements of leaf area index. Applied Optics, 34, 6211-6222.

Chen, J.M., Rich, P.M., Gower, S.T., Norman, J.M. and Plummer, 1 S., 1997. Leaf area index
2 of boreal forests - theory, techniques and measurements. J. Geophys. Res., 102(D24),
3 29429-29443.
4 Farque, L., Sinoquet, H. and Colin, F., 2001. Canopy structure and light interception in
5 *Quercus petraea* seedlings in relation to light regime and plant density. Tree Physiol.,
6 21, 1257-1267.
7 Hammer, Ø., Harper, D.A.T. and Ryan, P.D., 2001. PAST: Paleontological statistics software
8 package for education and data analysis. Palaeontologia Electronica, 4, 9 pp.
9 Jonckheere, I., Nackaerts, K., Muys, B. and Coppin, P., 2005. Assessment of automatic gap
10 fraction estimation of forests from digital hemispherical photography. Agric. Forest
11 Meteorol., 132, 96-114.
12 Koch, J.M. and Ward, S.C., 2005. Growth of jarrah (*Eucalyptus marginata*) on rehabilitated
13 bauxite mines in south-western Australia in thirteen years. Aust. Forestry, 68, 176-
14 185.
15 Kucharik, C.J., Norman, J.M. and Gower, S.T., 1998. Measurements of branch area and
16 adjusting leaf area index indirect measurements. Agric. Forest Meteorol., 91, 69-88.
17 Kucharik, C.J., Norman, J.M. and Gower, S.T., 1999. Characterization of radiation regimes in
18 nonrandom forest canopies: theory, measurements, and a simplified modeling
19 approach. Tree Physiol., 19, 695-706.
20 Lang, A.R.G. and Xiang, Y., 1986. Estimation of leaf area index from transmission of direct
21 sunlight in discontinuous canopies. Agric. Forest Meteorol., 35, 229-43.
22 Le Dantec, V., Dufrene, E. and Saugier, B., 2000. Interannual and spatial variation in
23 maimum leaf area index of temperate deciduous stands. For. Ecol. Manage., 134, 71- 81.
Leblanc, S.G., 2002. Correction to the plant canopy gap-size analysis 1 theory used by the

2 Tracing Radiation and Architecture of Canopies instrument. Applied Optics, 41, 7667-
3 7670.
4 Leblanc, S.G., 2006. Digital Hemispherical Photography Manual, Version 1.3b (10 August
5 2006). Canada Centre for Remote Sensing, Natural Resources Canada, Ottawa.
6 Leblanc, S.G., Chen, J.M., Fernandes, R., Deering, D.W. and Conley, A., 2005. Methodology
7 comparison for canopy structure parameters extraction from digital hemispherical
8 photography in boreal forests. Agric. Forest Meteorol., 129, 187-207.
9 Macfarlane, C., Coote, M., White, D.A. and Adams, M.A., 2000. Photographic exposure
10 affects indirect estimation of leaf area in plantations of *Eucalyptus globulus* Labill.
11 Agric. Forest Meteorol., 100, 155-168.
12 Macfarlane, C., Hoffman, M., Eamus, D., Kerp, N., Higginson, S., McMurtrie, R. et al., 2006.
13 Estimation of leaf area index in eucalypt forest using digital photography. Agric.
14 Forest Meteorol., accepted September 2006.
15 McArdle, B.H., 1988. The structural relationship: regression in biology. Can. J. Zool., 66,
16 2329-2339.
17 Menucuccini, M. and Grace, J., 1995. Climate influences the leaf area/sapwood area ratio in
18 Scots pine. Tree Physiol., 15, 1-10.
19 Snowden, P., 1986. Sampling strategies and methods of estimating the biomass of crown
20 components in individual trees of *Pinus radiata* D. Don. Aust. Forest Res., 16, 63-72.
21 Snowden, P., 1991. A ratio estimator for bias correction in logarithmic regressions. Can. J.
22 For. Res., 21, 720-724.
23 van Gardingen, P.R., Jackson, G.E., Hernandez-Daumus, S., Russell, G. and Sharp, L., 1999.
24 Leaf area index estimates obtained for clumped canopies using hemispherical
25 photography. Agric. Forest Meteorol., 94, 243-257.
Wagner, S., 1998. Calibration of grey values of hemispherical 1 photographs for image
2 analysis. Agric. Forest Meteorol., 90, 103-117.
3 Wagner, S., 2001. Relative radiance measurements and zenith angle dependent segmentation
4 in hemispherical photography. Agric. Forest Meteorol., 107, 103-115.
5 Wagner, S. and Hagemeier, M., 2006. Method of segmentation affects leaf inclination angle
6 estimation in hemispherical photography. Agric. Forest Meteorol., in press.
7 Ward, S.C. and Koch, J.M., 1995. Early growth of jarrah (*Eucalyptus marginata* Donn ex
8 Smith) on rehabilitated bauxite mines in south west Australia. Aust. Forestry, 58, 65-71.
10 Warton, D.I., Wright, I.J., Falster, D.S. and Westoby, M., 2006. Bivariate line-fitting models
11 for allometry. Biological Reviews, 81, 259-291.
12 Welles, J.M. and Norman, J.M., 1991. Instrument for indirect measurement of canopy

13 architecture. Agron. J., 83, 818-825.
14 Whitford, K.R., 1991. Crown assessments improve regression estimates of leaf area in jarrah
15 trees (*Eucalyptus marginata*). Aust. J. Bot., 39, 535-544.
16 Zhang, Y., Chen, J.M. and Miller, J.R., 2005. Determining digital hemispherical photograph
17 exposure for leaf area index estimation. Agric. Forest Meteorol., 133, 166-181.
18
28

Table 1. The range of tree heights, basal area (A_B) and leaf area index (L) of each stand estimated from destructive sampling.

Spacing (m)	Pit	Height (m)	A_B (m^2 ha^{-1})	L
1x1	KR	-	43.4	1.71
	ScR	3.9-9.2	47.7	1.66
	SN	3.3-10.6	66.7	2.75
2x2	KR	-	40.2	1.89
	ScR	9.0-14.1	56.2	2.72
	SN	9.6-12.8	56.8	2.83
4x2	KR	12.2-14.7	50.4	2.61
	ScR	8.1-14.0	38.9	1.94
	SN	9.2-12.4	44.9	2.31
4x4	KR	9.3-14.3	20.6	1.06
	ScR	6.9-13.8	16.8	0.85
	SN	8.2-13.9	31.2	1.73

Table 2. Ordinary least squares regressions (n = 35) of tree leaf area estimated from destructive sampling versus tree leaf area (LA) obtained from diameter at 1.3 m height under bark (DUB), crown width (CW), crown depth (CD) or Grimes density (GD) using selected equations from Whitford (1991). The correlation coefficient (R^2), significance of the regression (P), the significance of the t-test for slope ≠ 1, and root mean-squared error (RMSE) are also given. The 95 % confidence interval for all intercepts included zero except eq. iii. The single-stemmed equivalent DUB was used for forked trees.

Equation	Slope	Intercept	R^2	P	P (slope ≠ 1)	RMSE
(ii) $LA = 0.19 \times DUB^{1.73}$	0.95	-0.27	0.75	<0.001	0.62	5.6
(iii) $LA = 0.238 \times CW^{1.47} \times GD^{1.95}$	0.79	3.57	0.58	<0.001	0.08	7.6
(iv) $LA = 0.033 \times DUB^{1.45} \times GD^{1.71}$	0.92	-0.92	0.71	<0.001	0.34	6.9
(vii) $LA = 0.199 \times CD^{1.56} \times GD^{1.43}$	1.08	2.94	0.67	<0.001	0.54	7.4
(viii) $LA = 0.159 \times CD^{0.82} \times GD^{1.61} \times CW^{0.94}$	1.43	1.17	0.81	<0.001	0.001	7.5
(ix) $LA = 0.052 \times DUB^{1.02} \times GD^{1.76} \times CW^{0.55}$	0.86	1.80	0.71	<0.001	0.15	6.1

Table 3. Root mean-squared error of each fisheye photography method. θ is the zenith range used for the analyses, NC denotes no correction for foliage clumping, LX denotes the Lang-Xiang method, CC denotes the Chen-Cihlar method and CLX denotes the combined Lang-Xiang and Chen-Cihlar methods.

Software	gamma	image	θ	NC	LX	CC	CLX
PhotoShop	2.2	cover	0-15°	0.78		0.44	
WinSCANOPY	2.2	cover	0-15°	0.83		0.49	
WinSCANOPY	1.0	cover	0-15°	0.75		0.58	
DHP-TRACWin	1.0	circular fisheye	16-45°	0.95	0.72	0.75	0.50
DHP-TRACWin	1.0	circular fisheye	57°	0.90	0.77	0.74	0.54
WinSCANOPY	1.0	circular fisheye	0-70°	0.49	0.49	0.67	1.15
WinSCANOPY	2.2	circular fisheye	0-70°	0.51	0.46	0.55	0.75
WinSCANOPY	1.0	fullframe fisheye	0-70°	0.50	0.56	0.51	1.08
WinSCANOPY	2.2	fullframe fisheye	0-70°	0.54	0.43	0.49	0.57
Hemiview	1.0	circular fisheye	0-90°	0.73			
Hemiview	2.2	circular fisheye	0-90°	0.81			

Table 4. RMA regressions of plant area index L_t from photography versus leaf area index L from destructive sampling. The correlation coefficient (R^2) and significance of the regression (P) are given. An asterisk indicates intercepts whose 95 % confidence interval did not include zero and slopes that differed from one ($P < 0.05$).

clumping correction	gamma	a	b	R^2	P
$L_{t\ cover} = a\,L + b$					
CC (PhotoShop)	2.2	1.14	-0.12	0.69	<0.001
CC (WinSCANOPY)	2.2	1.27	-0.41	0.66	0.001
$L_{t\ fullframe} = a\,L + b$					
NC (WinSCANOPY)	1.0	0.82	0.085	0.58	0.004
LX (WinSCANOPY)	2.2	0.86	0.12	0.55	0.005
CC (WinSCANOPY)	2.2	0.67*	0.73*	0.45	0.018
$L_{t\ circular} = a\,L + b$					
NC (WinSCANOPY)	1.0	0.58*	0.62*	0.55	0.006
LX (WinSCANOPY)	2.2	0.69*	0.50*	0.59	0.004
LX (WinSCANOPY)	1.0	0.67	0.71*	0.41	0.026
CLX (DHP-TRACWin 16-45°)	1.0	0.71	0.46*	0.40	0.030

Table 5. The mean (for the three mine pits) and its standard error (sem) for each tree spacing of leaf area index (L) obtained from destructive sampling, plant area index (L_t) obtained from either fisheye or cover photography, and crown cover (f_C), foliage cover (f_F) crown porosity (Φ) and the zenithal clumping index ($\Omega(0)$) obtained from cover photography. The light extinction coefficient (k) was calculated from Equation 2.

Spacing		L	L_t[1]	L_t[2]	L_t[3]	$\Omega(0)$	f_C	f_F	Φ	k
1×1	mean	2.04	2.41	2.40	2.78	0.76	0.75	0.63	0.16	0.67
	sem	0.355	0.172	0.025	0.173	0.037	0.060	0.048	0.006	0.059
2×2	mean	2.48	2.20	2.02	2.48	0.65	0.61	0.53	0.15	0.47
	sem	0.298	0.157	0.083	0.302	0.022	0.067	0.062	0.007	0.031
2×4	mean	2.28	1.90	1.77	2.14	0.53	0.48	0.43	0.11	0.47
	sem	0.194	0.257	0.198	0.386	0.029	0.072	0.064	0.002	0.041
4×4	mean	1.21	1.25	1.35	1.21	0.48	0.28	0.24	0.12	0.46
	sem	0.266	0.431	0.245	0.347	0.038	0.095	0.079	0.011	0.044

[1] WinSCANOPY, fullframe images, gamma = 2.2, θ = 0-70°, LX method.

[2] DHP-TRACWin, circular images, gamma = 1.0, θ = 16-45°, CLX method.

[3] PhotoShop, cover images, gamma = 2.2, θ = 0-15°, CC method.

Table 6. RMA regressions of crown attributes obtained from PhotoShop (Y axis) and WinSCANOPY (X axis). All images were not corrected for the camera's gamma function (2.2). All regressions were significant to P < 0.0005. Asterisks indicate intercepts whose 95 % confidence interval did not include zero and slopes that differed from one (P<0.05, t-test). Four data points with zero cover were not analysed for crown porosity or clumping index regressions.

Crown attribute	n	Slope	Intercept	R^2
crown cover	138	1.02*	0.0156*	0.99
foliage cover	138	1.00	0.0190*	0.99
crown porosity	134	1.04	0.00236	0.48
clumping index	134	1.10*	-0.0347	0.85
leaf area index	138	0.932*	0.175*	0.95

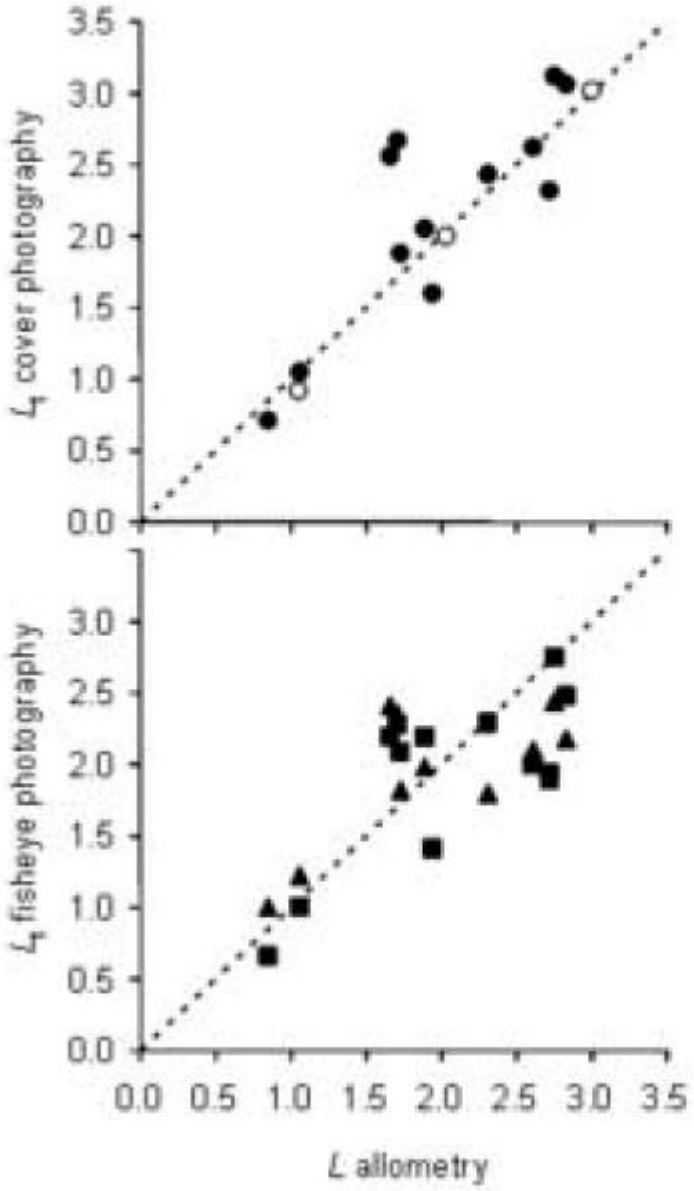
L_4 cover photography
L_4 fisheye photography
L allometry
0.0
0.5
1.0
1.5
2.0
2.5
3.0
3.5

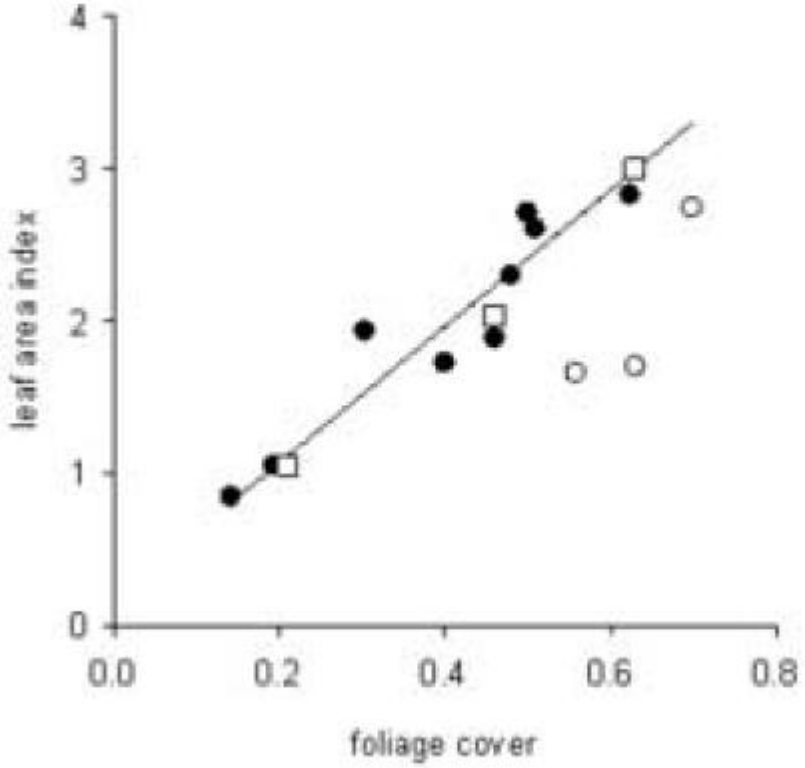
leaf area index
foliage cover
0
1
2
3
4
0.0
0.2
0.4
0.6
0.8

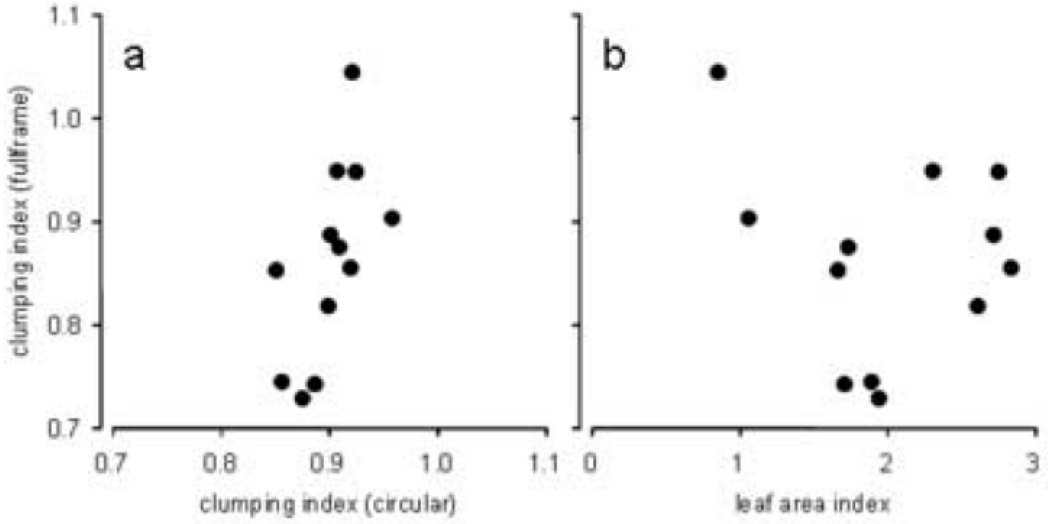
a
b
clumping index (fullframe)
clumping index (circular)
leaf area index
0.7
0.8
0.9
1.0
1.1
0
1
2
3

Figure 1. Plant area index L_t from cover and fisheye photography 1 *versus* leaf area index L
2 from allometry. For cover photography, data from PhotoShop are presented (filled circles)
3 together with data from Macfarlane et al. (2006, empty circles). For fisheye photography,
4 data from WinSCANOPY (filled squares, fullframe images with gamma = 2.2 and LX
5 clumping correction) and DHP-TRACWin (filled triangles, circular images with gamma =
6 1.0, θ = 16-45° and CLX clumping correction) are presented. See Table 3 for RMSE of the
7 regressions and Table 4 for regression data. Dashed line represents the 1:1 line.
8
9 Figure 2. Leaf area index estimated from destructive sampling and allometry *versus* foliage
10 cover from photography (from PhotoShop). The RMA regression equation was $L = 4.47\ f_f +$
11 0.18 (n = 12, $R^2 = 0.91$, $P < 0.001$) and included the data from Macfarlane et al. (2006, open
12 squares) but not the data from the 1×1 m spaced plots in the current study (open circles).
13 Data from the other treatments in the current study are represented by closed circles. The 95
14 % confidence interval of the intercept included zero.
15
16 Figure 3. a) The mean clumping index from circular and fullframe fisheye photography
17 (WinSCANOPY, gamma = 2.2), calculated as the ratio of L_t corrected for clumping using the
18 Lang-Xiang method to L_t uncorrected for foliage clumping. b) The clumping index from the
19 fullframe images (gamma = 2.2) *versus* LAI from destructive sampling.
20